RSC Advances

PAPER

View Article Online
View Journal | View Issue

Cite this: *RSC Adv.*, 2020, **10**, 1572

The function of oxybuprocaine: a *parachute* effect that sustains the supersaturated state of anhydrous piroxicam crystals†

Momoko Fujita,[a] Satoru Goto,[*ab] Hitoshi Chatani,[a] Yuta Otsuka,[ab] Yohsuke Shimada,[ab] Hiroshi Terada[ab] and Katsuyuki Inoo[c]

Received 28th November 2019
Accepted 17th December 2019

DOI: 10.1039/c9ra09952b

rsc.li/rsc-advances

Polymers have been recognized to have the function of sustaining the supersaturated state of drugs. This function has been widely studied because it will improve the absorption of poorly water-soluble drugs. However, clarifying the mechanism of this sustaining pharmaceutical effect (*parachute* effect) on the supersaturated state as a result of polymers is remains a task. We have found that oxybuprocaine, which is a small molecule, has a *parachute* effect on the supersaturated state (due to an anhydrate-to-hydrate transformation) of piroxicam-anhydrate in the aqueous phase. We consider that oxybuprocaine controls the environment of the solution and the network of polymers is unnecessary. Therefore, oxybuprocaine not only becomes a clue for elucidating the essential mechanism of the *parachute* effect of polymers but also enables us to rationally propose a new type of solubilizer.

1. Introduction

In the development of pharmaceuticals, for drugs that have polymorphs, it is necessary to select the most stable crystal form of the anhydrate or hydrate crystal. In most of the cases, the stable form has a lower solubility than the metastable form and this characteristic will affect the absorbability of the drug. Drugs in the metastable form can lead to problems such as redoing clinical trials due to the appearance of a more stable crystal form. There are several cases of failure in clinical trials and the collection after marketing due to the appearance of more stable crystals.[1–3] A representative example is ritonavir (product name: Norvir®), marketed as a semi-solid capsule formulation and liquid formulation by Abbott Laboratories.[1] For Norvir®, the crystal form 1 of ritonavir, considered to be the most stable crystal, had been used. However, the precipitation of a more thermodynamically stable and much less soluble crystalline, crystal form 2, had emerged in the final drug product. Therefore, it can be said that ritonavir was supersaturated in the product. If we could keep the metastable state stable, it will lead to the prevention of failure in the pharmaceutical development.

The supersaturated state has been widely studied because it has an advantage in the oral administration of drugs. Many studies have reported a variety of techniques that are used to supersaturate poorly water-soluble drugs.[4,5] Furthermore, apart from the generation of the supersaturation state, strategies that can maintain the state are required.[4] To maintain the supersaturated state, polymers are frequently used as additives which temporarily inhibit the precipitation by preventing nucleation and/or crystal growth.[6,7] However, clarifying the mechanism of the sustaining pharmaceutical effect (the *parachute* effect) on this supersaturated state by the polymers remains a task. We focused on how the additives affect supersaturation by using a drug which has an anhydrate-to-hydrate transformation (one of the simplest mechanisms of supersaturation).

Drugs capable of forming hydrates can cause anhydrate-to-hydrate transformation through dissolution.[8,9] The anhydrous form of drugs dissolves rapidly in the aqueous phase, leading to a supersaturated state, which means there is a temporarily higher concentration of the solution than the equilibrium concentration.[10] In supersaturated solutions, the dissolved drug molecules interact with water molecules and precipitate as a hydrate crystal. In this type of dissolution behavior, the equilibrium between the anhydrate crystal and solution changes to the equilibrium between monohydrate crystal and solution through supersaturation. This can be described as the reversible reactions shown below.[11]

$$\mathrm{A} \underset{k_{-1}}{\overset{k_{+1}}{\rightleftharpoons}} \mathrm{B} \underset{k_{-2}}{\overset{k_{+2}}{\rightleftharpoons}} \mathrm{C} \quad (1)$$

Here, A, B, and C represent anhydrate crystal, dissolved molecules in the solution, and the hydrate crystal, respectively. The

[a]Faculty of Pharmaceutical Sciences, Tokyo University of Science, 2641 Yamazaki, Noda, Chiba, 278-8510, Japan. E-mail: s.510@rs.tus.ac.jp; Tel: +814-7124-1501
[b]Research Institute for Science and Technology, Tokyo University of Science, 2641 Yamazaki, Noda, Chiba, 278-8510, Japan
[c]Teikoku Seiyaku Co., 567 Sanbonmatsu, Higashikagawa, Kagawa, 769-2695, Japan

† Electronic supplementary information (ESI) available. See DOI: 10.1039/c9ra09952b

dissolution and precipitation rate constants of the anhydrate crystal (A to B) are represented by k_{+1} and k_{-1}. The dissolution and precipitation rate constants of the hydrate crystal (B to C) are represented by k_{+2} and k_{-2}.

Oxicam structure-typed non-steroidal anti-inflammatory drugs (NSAIDs) are attracting attention because of the possibility that they may serve as potential therapeutic drugs to retard or terminate the progression of Parkinson's disease through their potent neuroprotective effect.[12] However, they are disadvantageous in terms of physicochemical properties, especially in aqueous solubility.[13,14] Piroxicam-anhydrate (PX-AH) has a low solubility as well as other oxicam-type NSAIDs, but it can achieve a supersaturated state in the aqueous phase temporarily due to the anhydrate-to-hydrate transformation before reaching the equilibrium state.[15–17] If this supersaturated state can be sustained, we can overcome the problem of a low aqueous solubility. For this reason, we chose PX-AH's dissolution behavior as the model of supersaturation.

We have previously reported the effect of structurally comparable local anesthetics (LAs) on the hydrophobicity and aqueous solubility of indomethacin, another NSAID.[18,19] LAs can be considered to also affect the dissolution behavior and solubility of PX. In this study, lidocaine (LID), tetracaine (TET), oxybuprocaine (OXY) and dibucaine (DIB) from the series of LAs were used as additives and the dissolution behavior changes of PX in the presence/absence of them were kinetically analyzed.

2. Experimental section

2.1. Materials

PX-AH, OXY hydrochloride, TET hydrochloride, DIB hydrochloride, sodium dihydrogen phosphate and disodium hydrogen phosphate were purchased from Wako Pure Industries (Osaka, Japan). Meloxicam (MX) and theophylline-anhydrate (THEO-AH) was obtained from Tokyo Chemical Industry Co. (Tokyo, Japan) and LID hydrochloride and dimethyl sulfoxide-d_6 (DMSO-d_6) supplied by Sigma-Aldrich Co. (St. Louis, MO, USA). All of the reagents used in this study were of the highest grade commercially available.

2.2. Solubility measurements

OXY hydrochloride, LID hydrochloride, TET hydrochloride, and DIB hydrochloride powders were dissolved in 0.025 M Na-phosphate buffer (pH 6.9) at various concentrations. Next, an excess amount of PX-AH (10 mg), MX (10 mg) or THEO-AH (40 mg) powder was added to screw-capped vials containing each solution (2 mL). The samples were shaken for 0 to 504 h at 25 °C using a BioShaker V BR-26 (TAITEC Corp., Saitama, Japan). For the mild conditions (slow stirring rate), a Water Bath Shaker PERSONAL-11 (TAITEC Corp., Saitama, Japan) was used. The liquid phase of the samples was subsequently diluted five times with the buffer and filtered through 0.22 μm polytetrafluoroethylene membrane filters. The concentrations of PX and MX in each sample were analyzed by high-performance liquid chromatography ultraviolet (HPLC-UV) spectroscopy. The HPLC system (Shimadzu Corp., Kyoto, Japan) consisted of an auto sampler (SIL-20A), a UV-vis detector (SPD-20A), a column oven (CTO-10AS VP), an online degasser (DGU20-A_3), and an HPLC pump (LC20-AD). The separation was conducted using an Almtackt Cadenza CD-C18 (100 × 3 mm, 3 μm) column with a flow rate of 0.35 mL min^{-1} at 40 °C. The column was a gift from Teikoku Seiyaku Co., Ltd. The mobile phase contained the buffer and HPLC-grade methanol in a volume ratio of 3 : 7 and the injection volume of each sample was 10 μL. The concentrations of PX, MX, and THEO were measured at the wavelengths 353 nm, 362 nm, and 271 nm, respectively.

2.3. Dissolution profile analysis

For the dissolution behavior that shows a supersaturated state, which follows eqn (1), we fitted the experimental data with eqn (2), and calculated the rate constants.[11]

$$y = \frac{k_{+1}k_{-2}}{\alpha\beta} - \frac{k_{-1}k_{+2} - k_{+1}\alpha}{(\beta-\alpha)\alpha}\exp(-\alpha t) + \frac{k_{-1}k_{+2} - k_{+1}\beta}{(\beta-\alpha)\alpha}\exp(-\beta t)$$

$$\alpha + \beta = k_{+1} + k_{-1} + k_{+2} + k_{-2}$$

$$\alpha\beta = k_{+1}k_{+2} + k_{+1}k_{-2} + k_{-1}k_{-2} \quad (2)$$

Here, k_{+1}, k_{-1}, k_{+2} and k_{-2} are rate constants that correspond to eqn (1) and t is the time (minute or hour). Dissolution profiles that did not show supersaturation were calculated by the Noyes–Whitney equation, as shown in eqn (3).[20]

$$C = C_s[1 - \exp(kSt)] + C_0\exp(-kSt) \quad (3)$$

Where k is the dissolution rate constant, S is the surface area, C is the concentration of the solute in time t, and C_s is the solubility in the equilibrium. C_0 is the concentration of the drugs from the initial release and not related to the release of the crystal.

2.4. Surface tension measurements

The surface tension was measured by applying the Du Noüy ring method. 0–5 mM LA solutions were prepared by 0.025 M Na-phosphate buffer (pH 6.9) and measured. The surface tension of each LA solution was relatively given from eqn (4).

$$\gamma = \gamma_w\frac{\theta}{\theta_w} \quad (4)$$

Here, γ is the surface tension of the sample and γ_w is the surface tension of water, which is already known as 72.00 mN m^{-1} at 25 °C.[21] θ and θ_w are the scale readings at the point when the ring breaks the surface of the sample and water, respectively.

2.5. Thermogravimetric (TG) analysis

TG analyses were conducted in air at a heating rate of 10 °C min^{-1} from 27 °C to 500 °C using a TG 8120 thermal analyzer (Rigaku Co., Tokyo, Japan). Al_2O_3 was used as the reference material.

2.6. Powder X-ray diffraction (PXRD) analysis

PXRD patterns were detected using a RINT 2000 X-ray diffractometer (Rigaku Co., Tokyo, Japan) with Cu-Kα as the X-ray source. The voltage and strength of the electric current were 40 kV and 40 mA, respectively. The samples were analyzed by a parallel beam method using cross-beam optics in a 2θ range of 5–40° at a scanning velocity of 0.02 steps.

2.7. Attenuated total reflectance-Fourier transform infrared (ATR-FTIR) spectroscopy

ATR-FTIR spectra were recorded on an FTIR spectrometer (PerkinElmer Co., Massachusetts, USA) equipped with a universal attenuated total reflectance accessory. At 25 °C, a 100 N force was applied to the samples and the spectra were scanned from 4000 cm^{-1} to 400 cm^{-1} at a resolution of 1 cm^{-1}.

2.8. ^{1}H-NMR spectrometry

^{1}H-NMR spectra were recorded using a 400 MHz spectrometer (JNM-EC400, JEOL Ltd., Tokyo, Japan). The samples were dissolved in DMSO-d_6 containing tetramethylsilane as an internal standard. The deuterated solvent provided the lock signal.

3. Results

3.1. *Parachute* effect of LAs on a supersaturated state of PX-AH in aqueous phase

3.1.1. Solubility-time profile of PX-AH. We first started by observing the characteristic dissolution behavior of PX-AH and compared it with that of THEO-AH, which is generally known to show a supersaturated state in its dissolution behavior due to the anhydrate-to-hydrate transformation. The change in the dissolution amount of PX-AH over time in the absence of LAs is shown in Fig. 1a. In the absence of LAs, PX-AH dissolved rapidly up to about 1.8 mM (supersaturated concentration) for 1 h, after which its concentration gradually decreased to about 0.65 mM (equilibrium concentration) The powder of PX-AH was white until it reached the maximum solubility at 1 h, after which a yellow solid precipitated gradually along with a decrease in its concentration. The precipitate was analyzed by TG analyzer, PXRD, and ATR-FTIR spectroscopy (Fig. S1–S3†). The molecular weight of piroxicam monohydrate (PX-MH) is 349.4 g mol^{-1} and the theoretical percentage of water in PX-MH is 5.15%. By TG analysis, we detected a 5.01% of mass loss at approximately 100 °C, which is almost the same as the theoretical percentage. The result of the PXRD analysis showed major peaks at 2θ = 10.22°, 12.02°, 18.54°, 21.52°, and 26.38°, which are the same as the pattern of the PX-MH structure with a reference code of CIDYAP indexed in the Cambridge Structural Database. These results suggest that the yellow precipitate was the PX-MH crystal.[22–25] From these results, it can be said that the concentration of PX decreased after it reached the maximum value because the equilibrium between the solution and PX-AH crystal shifts to the equilibrium between the solution and PX-MH crystal.

Fig. 1b is the dissolution profile of THEO-AH. We calculated the dissolution rates of PX-AH and THEO-AH from eqn (2) (Table 1). k_{+1}/k_{-1} of PX-AH and THEO-AH were 1.79×10^1 and 2.21×10^3 respectively. From these values, it is clear that PX-AH shows about two orders of magnitude slower dissolution than THEO-AH.

3.1.2. Solubility-time profile of PX-AH in the presence of LAs. As the dissolution behavior of PX-AH is clarified, we next added the LAs in the liquid phase and observed how the dissolution behavior of PX-AH is affected. The dissolved amount of PX in 5 mM LA solutions over time was measured to evaluate the effect of LAs on PX-AH's dissolution behavior. In the presence of four different LAs, each of the LAs showed different characteristic effects on the dissolution behavior of PX-AH (Fig. 1a). Except for DIB, LAs did not result in changes to the initial dissolution rate and supersaturated concentration.

Table 1 The values of k_{+1}/k_{-1} and k_{+2}/k_{-2} obtained from eqn (2)

	PX-AH	THEO-AH
k_{+1}/k_{-1}	1.79×10^1	2.21×10^3
k_{+2}/k_{-2}	2.70×10^{-2}	1.61×10^{-1}

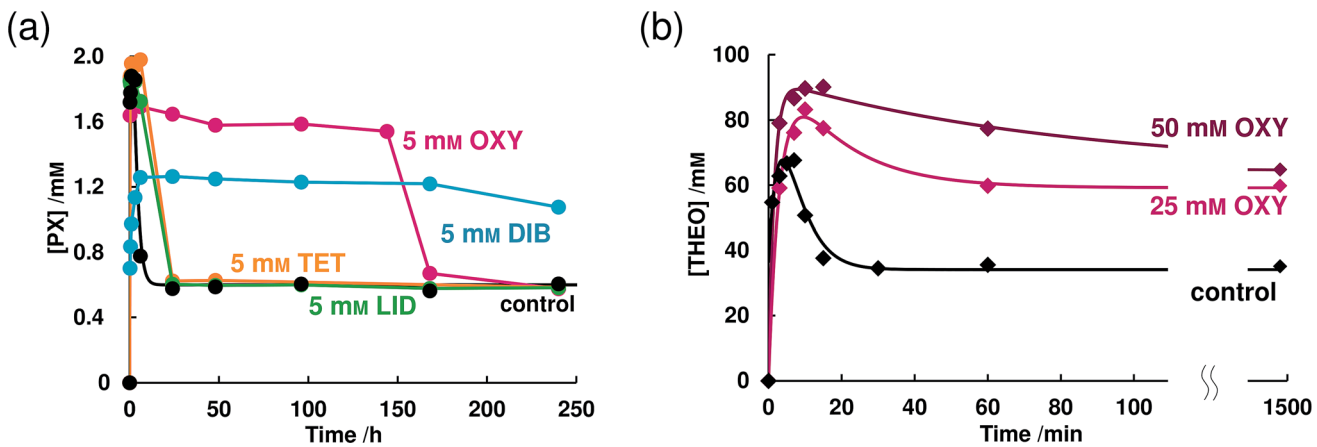

Fig. 1 The solubility–time profiles of (a) PX-AH and (b) THEO-AH in the absence and presence of LAs.

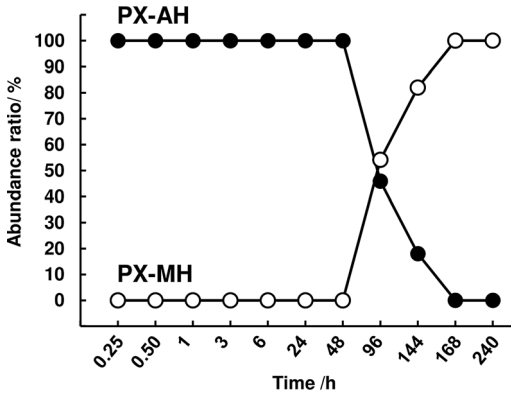

Fig. 2 The abundance rate of PX-AH and PX-MH calculated from the obtained ATR-FTIR spectra.

LID and TET gave no changes on the dissolution behavior of PX-AH. OXY sustained the supersaturated state of PX-AH for about 150 h (*parachute* effect) and then the concentration decreased to the equilibrium concentration of PX. This suggests that OXY has a *parachute* effect on PX-AH, though it is a small molecule. DIB decreased the initial dissolution rate of PX-AH and kept the concentration of about 1.2 mM for more than 240 h. From this result, we assume that DIB interacts with PX-AH more strongly than the other three LAs, which led to the decrease of the dissolution rate.

The solid phase of the samples when OXY exists was measured using FTIR (Fig. S4†). The abundance of PX-AH and PX-MH was calculated from the obtained spectra (Fig. 2). From this result, it can be seen that the *parachute* effect of OXY continues until the timing when the monohydrate crystal is formed (around 96–144 h).

The same experiment was conducted using THEO-AH. At a 5 mM concentration, OXY did not show its effect significantly on the dissolution behavior of THEO-AH. However, by increasing the concentration of OXY to 25 mM or more, increases of the supersaturated concentration and the equilibrium concentration were seen (Fig. 1b). From this result, it is clear that OXY acts specifically on PX-AH and maintains its supersaturated state. Putting together the results, the *parachute* effect on a supersaturated state of PX-AH is the specific feature of OXY that other LAs do not have and this does not work on the supersaturation state of THEO-AH.

3.1.3. Concentration dependence of LAs on the supersaturated concentration and equilibrium concentration of PX-AH. It was revealed in Section 3.1.2 that OXY at a concentration of 5 mM has a *parachute* effect on the supersaturated state of PX-AH. In this section, we varied the concentration of LAs and observed how the supersaturated concentration and the equilibrium concentration of PX-AH rely on the LA concentrations. OXY and TET from 0 to 50 mM and observed the changes of the supersaturated concentration (PX: 1 h, THEO: 3 min) and the equilibrium concentration (PX: 240 h, THEO: 1440 min). As the concentration of OXY and TET increased, both the supersaturated concentration and equilibrium concentration of THEO increased linearly (Fig. 3c and d). These results have no difference from the manner represented by sodium benzoate and caffeine.[26] However, for PX-AH, OXY decreased its supersaturated concentration as the concentration was increased (Fig. 3a). In addition, the equilibrium concentration hardly

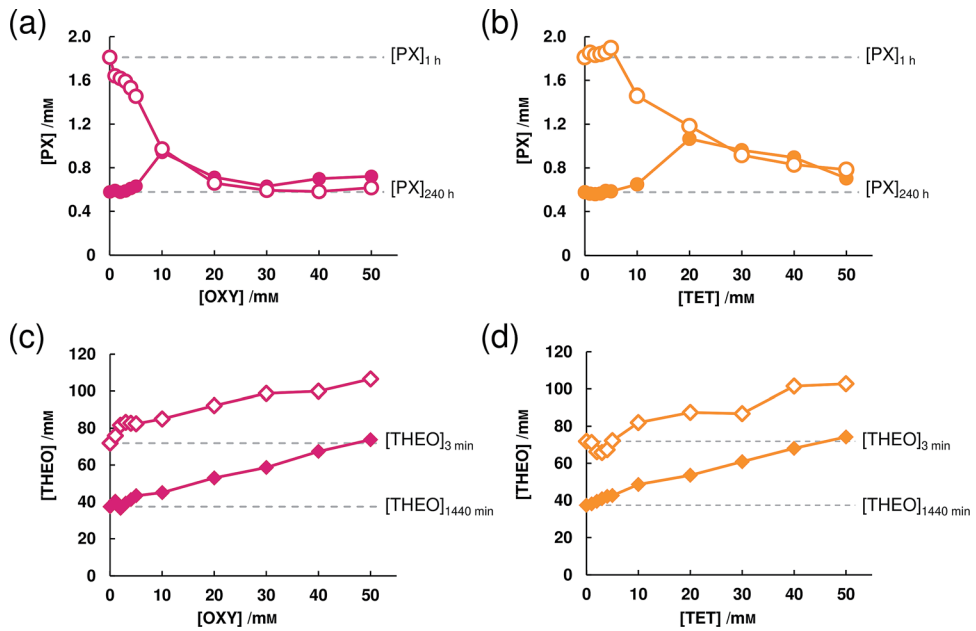

Fig. 3 Changes in the supersaturated concentrations and equilibrium concentrations of PX-AH and THEO-AH induced by various LA concentrations: the amount of PX-AH dissolved in various (a) OXY and (b) TET concentrated solutions at 1 h (supersaturated concentration, ○) and 240 h (equilibrium concentration, ●); the amount of THEO-AH dissolved in various (c) OXY and (d) TET concentrated solutions at 3 min (supersaturated concentration, ◇) and 1440 min (equilibrium concentration, ◆).

changed regardless of concentration of OXY. TET gave similar results (Fig. 3b).

3.2. Comparative study of LAs on the supersaturated state of PX-AH

3.2.1. Solubility-time profile of PX-AH in LA solutions in mild conditions. From Fig. 1a, it was clarified that though the four LAs are structurally similar, only OXY showed the *parachute* effect on the supersaturation state of PX-AH. To capture the unique characteristics of OXY, the dissolution studies were conducted under mild experimental conditions by decreasing the stirring rate compared to that of the experiments in Section 3.1. In addition, MX, which is also an oxicam-type NSAID, was also analyzed in comparison with PX-AH. The dissolved amount of PX or MX in 1 or 5 mM LA solutions over time was measured (Fig. 4a and b). In the 1 mM OXY, TET and DIB solutions, a decrease of the supersaturated concentration of PX was observed (Fig. 4a). Though the supersaturated concentration decreased, the equilibrium concentration did not change in any LA solutions.

In the 5 mM OXY solution, the concentration of PX slowly increased and reached a concentration of 1.74 mM at 504 h which is about the same value as the supersaturated concentration in the absence of LAs (Fig. 4b). In 5 mM TET and DIB solutions, a further decrease of supersaturated concentration than that of 1 mM was observed. TET did not change the equilibrium concentration but DIB hardly dissolved PX-AH. In both concentrations, LID did not have any effects on the dissolution behavior of PX-AH. The dissolution behavior of MX did not change regardless of the concentration of OXY, LID, or TET (Fig. 4c and d). In a 1 mM DIB solution, the decrease of the dissolution rate was observed and in a 5 mM DIB solution, MX hardly dissolved.

From the experiments in this section and Section 3.1.2, it became clear that LAs suppress the supersaturation of PX-AH but do not change the equilibrium concentration of PX. In addition, since MX does not have a supersaturated state in its dissolution behavior, the function of the LAs was not observed.

3.2.2. Surface tension of LA solutions. In Section 3.2.1, the supersaturation of PX-AH was suppressed by LAs. The phenomenon of suppression of the supersaturation by LAs may be acting on the process in which the solute molecules release from the anhydrate crystals towards the solution. Since this is dominated by the mass transfer in the interface between the solid phase (crystal) and the liquid phase (liquid), we considered the possibility of there being a relationship between the suppression of the supersaturation and the interfacial energy of the liquid phase side.[27] Hence, in this section, the surface tension was chosen for the parameter to evaluate the interfacial energy. The surface tension of LA solutions (0 to 5 mM) was measured and analyzed as to whether it has a relationship with the decrease of the supersaturated concentration (at 24 h) shown in Section 3.2.1. The surface tension decreased as the LA concentration increased (Fig. 5). We plotted $\Delta\gamma$ against $\Delta[PX]_{24\ h}$ and found that they had a high linear correlation of $R^2 = 0.9949$ (Table S1, Fig. S5†). The value of $\Delta\gamma$ was given from the difference in surface tension between a 5 mM LA solution and the buffer solution (control). $\Delta[PX]_{24\ h}$ is the value of how much

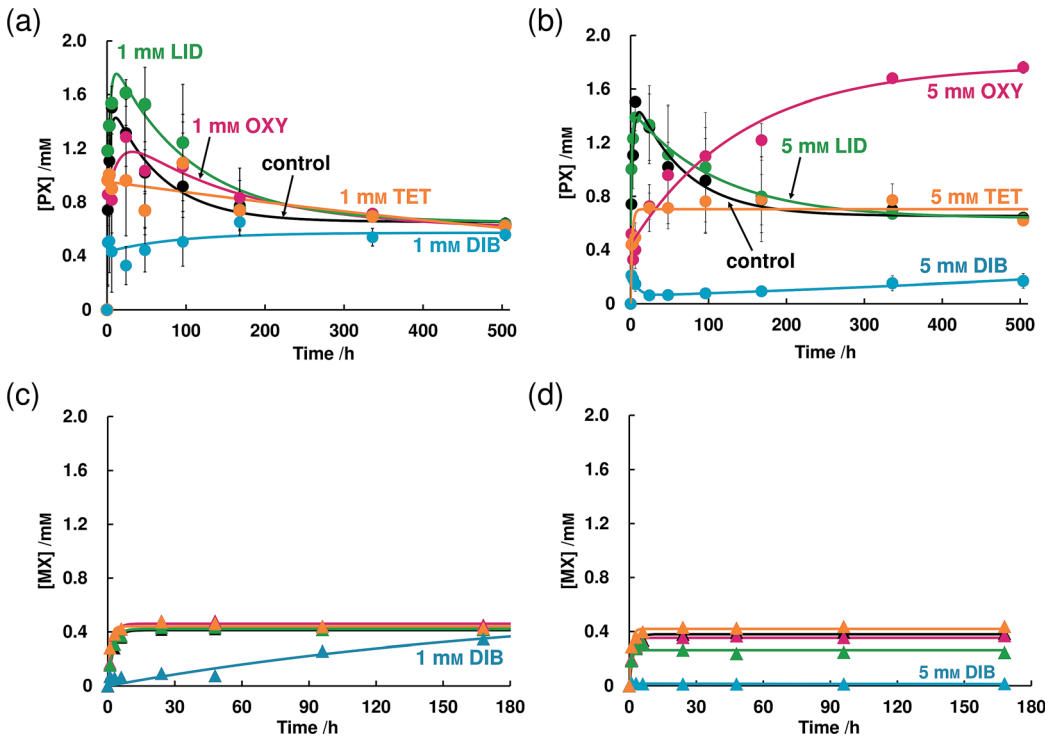

Fig. 4 The solubility–time profiles of PX-AH or MX in LA solutions under mild conditions: the dissolved amount of PX-AH over time in (a) 1 mM and (b) 5 mM LA solutions; the dissolved amount of MX over time in (c) 1 mM and (d) 5 mM LA solutions.

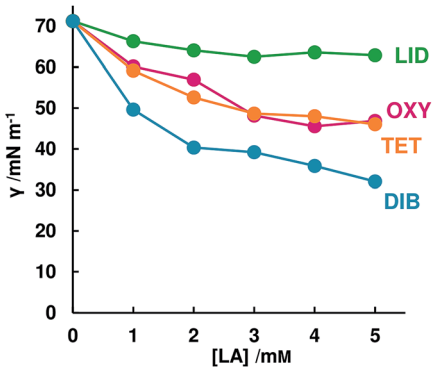

Fig. 5 The surface tension values of LA solutions.

the concentration of PX at 24 h decreased in 5 mM LA solutions compared to the buffer solution (given from the results in Section 3.2.1). This result suggests that the suppression of the supersaturation of PX-AH can be explained by the surface tension and this does not have a relationship with the *parachute* effect of OXY.

4. Discussion

The dissolution profile of PX-AH showed a much slower dissolution (about two orders of magnitude) than that of THEO-AH, which is generally known as a drug that occurs in the supersaturated state in the dissolution process. In this process, a crystal of PX-AH recrystallizes as a PX-MH crystal. In Section 3.2.1, it is revealed that, although the molecular structure of MX is similar to that of PX, MX did not show a supersaturated state in its dissolution profile. This may be due to its crystal stability and structural flexibility in solution. MX has a higher melting point and a higher crystalline density than PX, which are crucial factors that affects its crystal stability.[28–31] Furthermore, the difference in the molecular structures of PX and MX (PX has a 2-pyridinyl moiety whereas MX has a 5-methyl-2-thiazolyl moiety) can affect the structural stability of the drugs. It was reported that an intramolecular nonbonded interaction between sulfur and oxygen atoms observed in organosulfur compounds and the distance of nonbonded S···O atoms (3.32 Å) is significantly shorter than the sum of the corresponding van der Waals radii in a crystalline structure.[32] In addition, the molecules involved in this intramolecular nonbonded S···O interaction have a high structural-stability. In accordance with this report, we estimated the distance of the sulfur atom of the thiazolyl moiety and the oxygen atom of the amide in MX by the Gaussian 09 program at the B3LYP/cc-pVDZ level. As a result, the distance was 2.83 Å, which is shorter than the sum of the aforementioned van der Waals radii, which clearly shows that MX had intramolecular nonbonded 1,5-type S···O interactions. Taken together, conformation changes hardly occur in MX and a decrease in enthalpy cannot be expected even when MX forms a hydrate crystal. On the contrary, PX has a 2-pyridinyl moiety, which cannot interact intramolecularly and thus its 2-pyridinyl moiety can rotate. This means that the conformations of PX in solution are not uniform. However, with time, the dissolved PX molecules can gradually interact with water molecules and form a monohydrate crystal, the dissolution enthalpy of which is lower than that of an anhydrate crystal.

In Section 3.1.2, it is clearly shown that OXY has a *parachute* effect on the supersaturated state of PX-AH though OXY is a small molecule. It is generally known that hydrogels and polymer solutions can have a *parachute* effect on the supersaturated state.[6,33] We observed the Tyndall effect of the OXY solution including PX by shining the light on it. As shown in Fig. S6,† the Tyndall effect was not detected and found that the OXY solution did not form hydrogels. From this result and the dissolution studies, our work suggests that the network of polymers is unnecessary for *parachute* effect to occur in the supersaturated state of PX-AH. We have measured the dissolution behavior of PX-MH in 5 mM OXY solution and found that the OXY does not change its dissolution behavior nor equilibrium concentration (Fig. S7†). This result and the results in Fig. 2 clearly show that OXY increases the stabilization of the dissolved PX molecules in the solution and delays the precipitation of crystalline PX-MH. We have previously reported that at a high concentrated phosphate solution, a similar phenomenon occurs and the apparent water solubility changes with the structure of the solution.[34] Combined with this fact, OXY is thought to exhibit a *parachute* effect on the supersaturated state of PX-AH by modifying the interface to the solution of anhydrate crystal and monohydrate crystal.[37]

The results shown in Fig. 3a cannot enable us to predict how long the *parachute* effect of OXY continues depending on the concentration. Since the concentration of PX at 1 h decreased as the concentration of OXY increased, it can be considered that not only is there a disturbance of the association of the PX molecule and water molecule, but also more intricate interactions occur when the concentration of OXY is 10 mM or above. By putting this together with the results in Fig. 1a, 5 mM may become the optimal concentration for OXY to exert a *parachute* effect. Though TET did not show the *parachute* effect when at 5 mM (Fig. 1a), by comparing Fig. 3a and b, it can be predicted that TET will also show the *parachute* effect if we increase the concentration.

For THEO-AH, OXY increased both the supersaturated concentration and the equilibrium concentration, which had no specific difference with TET. Thus, this result suggests that both OXY and TET are working as a hydrotrope for THEO-AH.[35,36] Though OXY can be interpreted to work as a hydrotrope for PX-AH, we found that it has a *parachute* effect on the supersaturated state in a much lower concentration than in the conventional reports by A. M. Saleh *et al.* and J. Y. Kim *et al.*

By comparing the effect of DIB between the results of Fig. 1a (high stirring rate, *i.e.* the solid–liquid interface can be neglected) and Fig. 4b (slow stirring rate), it is clear that DIB strongly interacts with PX-AH in the solid–liquid interface and prevents PX-AH dissolving. Other LAs do not interact as strongly as DIB but affect the dissolution rate of PX-AH. How strong LAs interact with PX in the interface could be described with the surface tension because of having a high relationship with the dissolution amount at 24 h.

We have measured the NMR spectra and the FT-IR spectra of PX/OXY, PX/LID and PX/DIB mixtures in equimolar amounts. The results suggested that the proton of –OH in PX and MX and the nitrogen atom of the tertiary amine in OXY, LID, and DIB interact electrostatically (Fig. S8 and S9†).[37–41] From these results, it is considered that the *parachute* effect of OXY against the PX-AH's supersaturated state is not a simple system that interacts 1 : 1, but more intricate interactions among PX, OXY, and water molecules occur. However, since OXY molecules are smaller and simpler than the polymers, we can contribute to the elucidation of the mechanism of the *parachute* effect on the supersaturated state.

5. Conclusions

In this study, we found that each of the LAs has different characteristic effects on the dissolution behavior of PX-AH. Above all, a new function of OXY, a *parachute* effect on the supersaturated state of PX-AH, was clarified. Our results imply that it is possible for small molecules to have a *parachute* effect, and the network of polymers is unnecessary. Because OXY is a small molecule having much more simple properties than that of polymers, it may become a clue for understanding the essential mechanism of the *parachute* effect. Moreover, this finding may solve the problem of PX having low water solubility and suggests the possibility of a further increase in its usefulness as a treatment for Parkinson's disease.

Conflicts of interest

There are no conflicts to declare.

Acknowledgements

A part of this research was supported by a Research Grant for Young Scientists from the Faculty of Pharmaceutical Sciences, Tokyo University of Science. This work was partly supported by JSPS KAKENHI Grant Number 17K05366.

Notes and references

1 S. R. Chemburkar, J. Bauer, K. Deming, H. Spiwek, K. Patel, J. Morris, R. Henry, S. Spanton, W. Dziki, W. Porter, J. Quick, P. Bauer, J. Donaubauer, B. A. Narayanan, M. Soldani, D. Riley and K. McFarland, *Org. Process Res. Dev.*, 2000, **4**, 413–417.
2 B. Rietveld and R. Céolin, *J. Pharm. Sci.*, 2015, **104**, 4117–4122.
3 A. Q. P. Garbuio, T. Hanashiro, B. E. O. Markman, F. L. A. Fonseca, F. F. Perazzo and P. C. P. Rosa, *J. Appl. Pharm. Sci.*, 2014, **4**, 1–7.
4 K. T. Savjani, A. K. Gajjar and J. K. Savjani, *ISRN Pharm.*, 2012, **2012**, 1–10.
5 P. Gao and Y. Shi, *AAPS J.*, 2012, **14**, 703–713.
6 J. Brouwers, M. E. Brewster and P. Augustijns, *J. Pharm. Sci.*, 2009, **98**, 2549–2572.
7 N. J. Babu and A. Nangia, *Cryst. Growth Des.*, 2011, **11**, 2662–2679.
8 H. Nogami, T. Nagai and T. Yotsuyanagi, *Chem. Pharm. Bull.*, 1969, **17**, 499–509.
9 H. Wikström, J. Rantanen, A. D. Gift and L. S. Taylor, *Cryst. Growth Des.*, 2008, **8**, 2684–2693.
10 E. Shefter and T. Higuchi, *J. Pharm. Sci.*, 1963, **52**, 781–791.
11 H. Gutfreund, *Kinetics for the Life Science: Receptors, Transmitters and Catalysis*, Cambridge University Press, Cambridge, 1995, vol. 4, pp. 114–119.
12 Y. Tasaki, J. Yamamoto, T. Omura, T. Noda, N. Kamiyama, K. Yoshida, M. Satomi, T. Sakaguchi, M. Asari, T. Ohkubo, K. Shimizu and K. Matsubara, *Eur. J. Pharmacol.*, 2012, **676**, 57–63.
13 G. L. Amidon, H. Lennernäs, V. P. Shah and J. R. Crison, *Pharm. Res.*, 1995, **12**, 413–420.
14 N. Seedher and S. Bhatia, *AAPS PharmSciTech*, 2003, **4**, 26–44.
15 J. Jinno, D. M. Oh, J. R. Crison and G. L. Amidon, *J. Pharm. Sci.*, 2000, **89**, 268–274.
16 K. Tsinman, A. Avdeef, O. Tsinman and D. Voloboy, *Pharm. Res.*, 2009, **26**, 2093–2100.
17 H. Qu, T. Munk, C. Cornett, J. X. Wu, J. P. Bøtker, L. P. Christensen, J. Rantanen and F. Tian, *Pharm. Res.*, 2011, **28**, 364–373.
18 R. Tateuchi, N. Sagawa, Y. Shimada and S. Goto, *J. Phys. Chem. B*, 2015, **119**, 9868–9873.
19 Y. Shimada, R. Tateuchi, H. Chatani and S. Goto, *J. Mol. Struct.*, 2018, **1155**, 165–170.
20 A. A. Noyes and W. R. Whitney, *J. Am. Chem. Soc.*, 1897, **19**, 930–934.
21 M. A. Floriano and C. A. Angell, *J. Phys. Chem.*, 1990, **94**, 4199–4202.
22 J. Bordner, J. A. Richards, P. Weeks and E. B. Whipple, *Acta Crystallogr., Sect. C: Cryst. Struct. Commun.*, 1984, **40**, 989–990.
23 P. Taddei, A. Torreggiani and R. Simoni, *Biopolymers*, 2001, **62**, 68–78.
24 F. Vrečer, M. Vrbinc and A. Meden, *Int. J. Pharm.*, 2003, **256**, 3–15.
25 L. Y. Lyn, H. W. Sze, A. Rajendran, G. Adinarayana, K. Dua and S. Garg, *Acta Pharm.*, 2011, **61**, 391–402.
26 T. Higuchi and D. A. Zuck, *J. Am. Pharm. Assoc.*, 1953, **42**, 132–138.
27 J. Szekely and V. Stanek, *Chem. Eng. Sci.*, 1969, **24**, 11–24.
28 Drugbank, https://www.drugbank.ca/drugs/DB00554, accessed November 2019.
29 Drugbank, https://www.drugbank.ca/drugs/DB00814, accessed November 2019.
30 B. Kojić-Prodić and Ž. Ruž'ć-Toroš, *Acta Crystallogr., Sect. B: Struct. Crystallogr. Cryst. Chem.*, 1982, **38**, 2948–2951.
31 P. Luger, K. Daneck, W. Engel, G. Trummlitz and K. Wagner, *Eur. J. Pharm. Sci.*, 1996, **4**, 175–187.
32 Y. Nagao, T. Hirata, S. Goto, S. Sano, A. Kakehi, K. Iizuka and M. Shiro, *J. Am. Chem. Soc.*, 1998, **120**, 3104–3110.
33 G. C. R. M. Schver and P. I. Lee, *Mol. Pharm.*, 2018, **15**, 2017–2026.

34 H. Chatani, S. Goto, H. Kataoka, M. Fujita, Y. Otsuka, Y. Shimada and H. Terada, *Chem. Phys.*, 2019, **525**, 110415.
35 A. M. Saleh and L. K. El-Khordagui, *Int. J. Pharm.*, 1985, **24**, 231–238.
36 J. Y. Kim, S. Kim, M. Papp, K. Park and R. Pinal, *J. Pharm. Sci.*, 2010, **99**, 3953–3965.
37 H. Kataoka, Y. Sakaki, K. Komatsu, Y. Shimada and S. Goto, *J. Pharm. Sci.*, 2017, **106**, 3016–3021.
38 C. Rossi, A. Casini, M. P. Picchi, F. Laschi, A. Calabria and R. Marcolongo, *Biophys. Chem.*, 1987, **27**, 255–261.
39 V. Tantishaiyakul, S. Songkro, K. Suknuntha, P. Permkum and P. Pipatwarakul, *AAPS PharmSciTech*, 2009, **10**, 789–795.
40 Y. Umeda, T. Fukami, T. Furuishi, T. Suzuki, M. Makimura and K. Tomono, *Chem. Pharm. Bull.*, 2007, **55**, 832–836.
41 G. Yener, M. Üner, Ü. Gönüllü, S. Yildrim, P. Kiliç, S. S. Aslan and A. Barla, *Chem. Pharm. Bull.*, 2009, **58**, 1466–1473.